

Spatiotemporal Changes in Extreme Wet and Dry Conditions and Linkages with Planetary Oscillations

Authors: Li, Ying, Huang, Shengzhi, Ma, Lan, Huang, Qiang, Wu, Lianzhou, et al.

Source: Journal of Coastal Research, 84(sp1) : 134-143

Published By: Coastal Education and Research Foundation

URL: <https://doi.org/10.2112/SI84-019.1>

BioOne Complete (complete.BioOne.org) is a full-text database of 200 subscribed and open-access titles in the biological, ecological, and environmental sciences published by nonprofit societies, associations, museums, institutions, and presses.

Your use of this PDF, the BioOne Complete website, and all posted and associated content indicates your acceptance of BioOne's Terms of Use, available at www.bioone.org/terms-of-use.

Usage of BioOne Complete content is strictly limited to personal, educational, and non - commercial use. Commercial inquiries or rights and permissions requests should be directed to the individual publisher as copyright holder.

BioOne sees sustainable scholarly publishing as an inherently collaborative enterprise connecting authors, nonprofit publishers, academic institutions, research libraries, and research funders in the common goal of maximizing access to critical research.

Spatiotemporal Changes in Extreme Wet and Dry Conditions and Linkages with Planetary Oscillations

Ying Li[†], Shengzhi Huang[†], Lan Ma[†], Qiang Huang[†], Lianzhou Wu[†], Beibei Hou[†], and Guoyong Leng[‡]

[†]State Key Laboratory of Eco-hydraulics in Northwest Arid Region
Xi'an University of Technology
Xi'an, China

[‡]Environmental Change Institute
University of Oxford
Oxford, U.K.



www.cerf-jcr.org



www.JCRonline.org

ABSTRACT

Li, Y.; Huang, S.; Ma, L.; Huang, Q.; Wu, L.; Hou, B., and Leng, G., 2018. Spatiotemporal changes in extreme wet and dry conditions and linkages with planetary oscillations. *In: Wang, D. and Guido-Aldana, P.A. (eds.), Select Proceedings from the 3rd International Conference on Water Resource and Environment (WRE2017). Journal of Coastal Research, Special Issue No. 84, pp. 134-143. Coconut Creek (Florida), ISSN 0749-0208.*

Exploration of the spatiotemporal changes in extreme wet and dry events and their linkages with planetary oscillations is highly necessary for regional hazards mitigation. In this study, a standardized Surface Humid Index was applied for characterizing extreme dry and wet conditions (hereafter referred to as EDWC) in the Wei River Basin (WRB), China. Then, the heuristic segmentation method was adopted to determine the stationarity of extreme dry and wet frequency. The cross wavelet transform and coherence were used to reveal the linkages between EDWC and planetary oscillations. Results indicated that: (1) the standardized Surface Humid Index in the WRB has a striking trend towards wetter condition in summer and winter, whilst that in spring and autumn has a marked trend towards drier condition; (2) the northern basin has the highest extreme wet frequency, while the western basin has the lowest extreme dry and wet frequency; (3) the stationarity of the extreme dry and wet frequency series in the WRB is valid; (4) the planetary oscillations strongly affect the EDWC in the WRB. El Niño Southern Oscillation exhibits the strongest impacts on its EDWC, while Atlantic Multidecadal Oscillation shows the weakest impacts on its EDWC.

ADDITIONAL INDEX WORDS: *Extreme dry and wet events, large-scale atmospheric circulation patterns, ENSO, standardized Surface Humid Index, the cross wavelet analysis.*

INTRODUCTION

Recently, the global climate has experienced a noticeable variation, particularly for the global warming, which results in boosting the water circulation rate, thus the frequency of extreme conditions are increasing on the global scale (Beniston and Stephenson, 2004; Liu *et al.*, 2018; Su, Gemmer, and Jiang, 2008; Zheng *et al.*, 2006). The effects of these hazards on society are increasing and the socioeconomic developments tend to be more and more vulnerable (Fang *et al.*, 2017; Huang *et al.*, 2014c). For example, in the United States, the mid-west drought in 1988-1989 led to nearly \$39 billion economic losses. In 1992, Hurricane Andrew in South Florida in 1992 caused about \$30 billion economic losses, and the mid-west flood in 1993 resulted in approximately \$19 billion economic losses (Easterling *et al.*, 2000).

In view of the potentially devastating impacts of climate extremes, increasing attention to climate extremes has therefore been drawn to examine long-term trends of seasonal and annual climate variations of precipitation, temperature, precipitation and temperature extremes (Fang *et al.*, 2018; Jones and Moberg, 2003; Wang *et al.*, 2013). Previous studies have suggested that the intensity and frequency of extreme climate change are powerful indicators of climate change, and that the impact on nature and human society is far greater than that of average (Katz and Brown, 1992; Plummer *et al.*, 1999).

Extreme dry and wet events (hereafter referred to as EDWE) emerge after a prolonged deficit or obvious excessive rainfall, but determining the onset, termination as well as spatial extent of them is complicated. Based on this, numerous efforts have been paid to develop indicators for dry/wet monitoring and analysis (Trenberth *et al.*, 2014; Vicente-Serrano, Beguería, and López-Moreno, 2010a). Recently, some objective indicators like Palmer drought severity index (PDSI) as well as standardized precipitation index (SPI) (McKee, Doesken, and Kliest, 1993; Palmer, 1965) have been widely applied in dry/wet quantification and monitoring. Although the probabilistic feature of SPI makes it possible to directly compare various variables and locations (McKee, Doesken, and Kliest, 1993), SPI has an evident disadvantage, that is, only on the basis of precipitation; other key variables like temperature are not included. As a result, SPI cannot reflect the strong influences of evapotranspiration on dry/wet conditions (Tao *et al.*, 2014). Regarding PDSI, it is based on the concept of supply and demand, which contains prior precipitation, evaporation demand and humidity supply to characterize dry/wet conditions. However, some drawbacks of the PDSI exist. For instance, the water balance model is not strongly robust, and its numerical value is very short in both statistical and physical sense (Ma *et al.*, 2015). In the present study, a Standardized Surface Humid Index was utilized to characterize dry and wet conditions (Cao *et al.*, 2014; Zhang *et al.*, 2013), which incorporates rainfall and evapotranspiration and can generally overcome the shortcomings of SPI and PDSI to some extent.

Variations of climate extremes exhibited substantial regional

DOI: 10.2112/SI84-019.1 received 17 November 2017; accepted in revision 20 April 2018.

*Corresponding author: huangshengzhi7788@126.com

©Coastal Education and Research Foundation, Inc. 2018

discrepancies because the effects of climate change differ on various geographical regions (Guo *et al.*, 2013; Wang, Jiao, and Xin, 2013). The Wei River Basin (WRB), the study area in the present study, is the transitional region from a semi-humid region to an arid region. Located in a typical continental monsoon climate zone, the WRB is frequently assaulted by EDWE (Huang *et al.*, 2014a, 2015b). These bipolar extreme events are expected to increase risk and vulnerability of extremes to human populations highly rapidly in a nonlinear manner and reduce the efficiency of local water resources management (Reza, Ali, and Donald, 2016). The WRB is vital to China, especially the establishment of a national key economic development zone (the Guanzhong-Tianshui Economic Zone), which is conducive to the rapid economic development in Western China. Nevertheless, the high-frequency EDWE have adverse effects on local social and economic developments. Therefore, it is crucial to probe the spatiotemporal variations of the extreme wet and dry conditions in the WRB, which makes for local disaster reductions and water resource management (Zhang *et al.*, 2015a,b). Previous studies mainly focused on long-term trends of precipitation and temperature variations at annual and seasonal scales (Huang *et al.*, 2016b; Zhao *et al.*, 2015a,b). However, the spatial-temporal variations of the EDWE in the WRB have not been investigated well. Thus, one objective of this study is to fill this gap through fully exploring the spatiotemporal changes in the extreme wet and dry conditions in the WRB.

The distribution and intensity of extreme dry and wet conditions (hereafter referred to as EDWC) are strongly irregular in spatiotemporal dimensions (Guo *et al.*, 2013). Climate indicators such as the Atlantic Multidecadal Oscillation (AMO), El Niño Southern Oscillation (ENSO), North Atlantic Oscillation (NAO), and Pacific Decadal Oscillation (PDO) can explain this phenomenon to a certain extent (Kam, Sheffield, and Wood, 2014; Kiem and Verdon-Kidd, 2009; Sabziparvar *et al.*, 2011; Talaei, Tabari, and Ardakani, 2014). Since the WRB is located in a typical continental monsoon climate zone, the large-scale atmospheric circulation patterns including AMO, ENSO, PDO, and NAO may have a strong impact on the change characteristics of its EDWE. Thus, it is very necessary to explore the correlations between local EDWE and planetary oscillations, which helps to reveal possible mechanism responsible for the variations of EDWE in the WRB, thus being helpful for establishing an early-warning EDWE system and effectively guiding local hazards mitigation. Therefore, another goal of this paper is to reveal the links between local EDWE and AMO, ENSO, PDO and NAO.

The major objectives of this study are (1) to examine the spatiotemporal changes in extreme wet and dry events in the WRB; (2) and to explore the correlations between local EDWE and AMO, ENSO, PDO, and NAO.

STUDY AREA AND DATA

The WRB was selected as a case to study. The detailed introduction on the WRB and data is shown as follows.

WRB

The WRB chosen as a case study in this current study is the longest tributary of the Yellow River in China (Figure 1). The

elevation gradually increases from the southeast to the northwest in this region. Its average annual precipitation is roughly 560 mm (Zhang *et al.*, 2008). However, the annual precipitation in the WRB varies distinctly owing to the north Pacific subtropical high intensity, duration and impact area of the unstable characteristics, which shows a strong impact on local precipitation, being expected to cause very frequent EDWE (Huang *et al.*, 2015c). Additionally, its precipitation has a marked seasonality, and that in flood period (from June to September) occupies nearly 60% of annual rainfall. Given the adverse effects of EDWE on local social and economic developments, it is very essential for us to investigate the spatiotemporal changes in extreme wet/dry conditions in the WRB and their linkages with large-scale atmospheric circulation patterns, which helps to effectively guide local hazards mitigation.

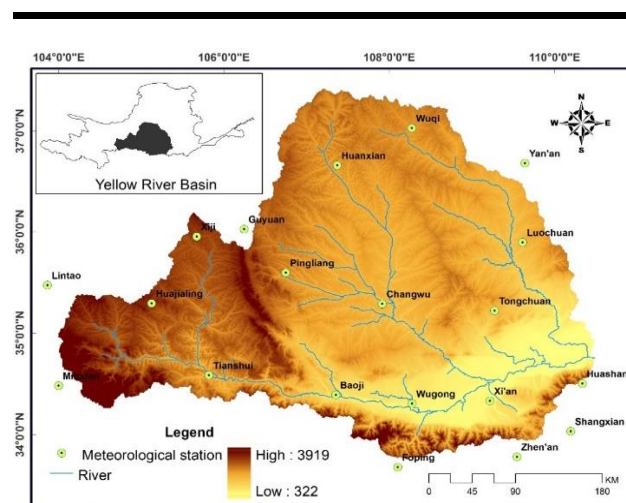


Figure 1. The locations of the WRB and the distribution of relevant meteorological stations.

Data

Daily precipitation, wind speed, relative humidity, sunshine hours, maximum, minimum and mean air temperature, as well as absolute vapour pressure data collected from 21 meteorological stations in this basin and its adjacent areas were adopted in this present study (Figure 1). Every station has the daily meteorological data spanning from January 1, 1960 to December 31, 2010, which were derived from National Climate Center (NCC) in China Meteorological Administration (CMA). Daily potential evaporation was computed through the Penman-Monteith formulation (Monteith, 1965). In addition, monthly AMO, PDO, ENSO, and NAO data spanning 1960-2010 were also adopted in this present study. Monthly PDO and AMO time series were acquired from the Tokyo Climate Center (http://ds.data.jma.go.jp/tcc/tcc/products/el_nino/decadal/pdo.html) and the National Oceanic and Atmospheric Administration (NOAA) Earth System Research Laboratory (<http://www.esrl.noaa.gov/psd/data/correlation/amon.us.long.dat>

a), respectively. For ENSO, the Nino 3.4 Index time series acquired from the NOAA Earth System Research Laboratory (<http://www.esrl.noaa.gov/psd/data/correlation/nina34.data>) was used in this study. Regarding NAO, its monthly data were acquired from the NOAA National Climatic Data Center (<http://www.ncdc.noaa.gov/teleconnections/ao.php>).

METHODS

This section briefly presents methods utilized in this study, among which a standardized Surface Humid Index is applied for characterizing extreme dry and wet conditions, followed by the modified Mann-Kendall trend test method for identifying the trends of Surface Humid Index. In addition, the heuristic segmentation method is adopted to determine the stationarity of extreme dry and wet frequency, and the cross wavelet transform and coherence are used to reveal the linkages between EDWC and planetary oscillations.

Surface Humid Index

Considerable indices for analyzing climate extremes have been developed aimed at monitoring and predicting the changes in precipitation and temperature with various time steps or spatial scales, including Crop Moisture Index (Palmer, 1965), Crop-Specific Drought Index (Meyer, Hubbard, and Wilhite, 1993), daily Water Stress Index (Jones and Moberg, 2003), and Soil Moisture Deficit Index (Narasimhan and Srinivasan, 2005). Especially Surface Humid Index has been extensively applied to characterize dry and wet conditions with monthly time step at global or regional scales (Ma and Fu, 2001). Surface Humid Index (H) is defined as the ratio of precipitation (P) to reference evapotranspiration (ET₀), which is expressed as follows:

$$H = \frac{P}{ET_0} \quad (1)$$

where, P denotes monthly precipitation; ET₀ represents monthly potential evaporation.

Extreme wet events are defined as the monthly standardized Surface Humid Index (H) larger than or equal to 0.5 (Cao *et al.*, 2014; Ma, Hua, and Ren, 2003). Extreme dry events are defined as the standardized H smaller than or equal to -0.5 (Zhang *et al.*, 2013, 2015a,b). Its calculation is expressed as follows:

$$D_{H_{ij}} = \frac{H_{ij} - \bar{H}_i}{\sigma_i} \quad (2)$$

where, H_{ij} represents the monthly H of the i-th month in the j-th year; H_i denotes the average H of the i-th month in the previous 51 years; and σ_i stands for the standard deviation of H of the i-th month.

The Modified Mann-Kendall Trend Test Method (MMK)

The traditional Mann-Kendall (MK) trend test approach is a nonparametric method. Nevertheless, the results of MK tend to be influenced by the persistence of time series (Huang *et al.*, 2014a). Hence, Hamed and Rao (1998) improved it via taking the lag-i autocorrelation into account to get rid of the persistence. Therefore, the MMK was applied to calculate the trends of monthly standardized Surface Humid Index series and extreme dry and wet conditions in the WRB (Hamed and Rao, 1998). The specific counting processes would be referred to Huang *et al.* (2014c).

The Heuristic Segmentation Method

Traditional statistical test methods of detecting the highly change points of time series rely on the assumption that the given time series should be stationary and linear. However, it is very difficult for these previous methods to accurately identify their real change points since some hydrological time series shows nonlinear and nonstationary characteristics (Huang *et al.*, 2015a, 2016a). The heuristic segmentation method proposed by Pedro, Plamen, and Lu *et al.* (2001) is based on the sliding T test. However, it is modified and extended to detecting change points in nonlinear and nonstationary time series. Nonstationary time series is divided into several stationary subseries in the heuristic segmentation method, and it can get rid of the drawbacks of aforementioned traditional methods (Pedro, Plamen, and Lu *et al.* 2001).

The conventional frequency analysis of extreme dry and wet events is relied on the stationarity assumption (Verdon-Kidd and Kiem, 2015), which indicates historical characteristics of extreme events can be extended to the future. However, the changing environment might change the statistical characteristics of hydroclimate time series, leading to so-called non-stationarity (Liu *et al.*, 2017). Neglecting the non-stationarity would therefore result in severe biases in assessing extreme events (Jiang *et al.*, 2014). Therefore, the heuristic segmentation method was adopted to identify the stationarity of extreme dry and wet events in the WRB. The detailed calculation processes would be referred to Huang *et al.* (2016a).

Cross Wavelet Transform and Coherence

The cross wavelet transform is a new method of revealing the correlations between two related time series (Grinsted, Moore, and Jevrejeva, 2004; Hudgins, Friehe, and Mayer, 1993). Using wavelet transform to combine the cross-spectrum analysis, two time series can be well reflected in the changing characteristics and the coupled oscillations both in time-frequency domain (Torrence and Compo, 1998). Wavelet coherence examines the regions with high common power, which is an approach for investigating how coherent the wavelet coherence in time and frequency domain. Therefore, in this present study, they are used to examine the correlations between the dry/wet conditions in the WRB and the large-scale atmospheric circulation patterns such as AMO, ENSO, PDO, and NAO. The detailed calculation processes can be referred to Torrence and Compo (1998).

RESULTS

The result section analyses the spatio-temporal changes in monthly standardized Surface Humid Index and the stationarity of the extreme dry and wet frequency series. Meantime, evidence is provided that the planetary oscillations affect the EDWC in the WRB.

Spatio-Temporal Changes in Monthly Standardized Surface Humid Index Series

The MMK was used to compute the trends of monthly standardized Surface Humid Index series at 21 meteorological stations in the basin (Huang *et al.*, 2014a). In terms of MMK statistics, when their absolute values are larger than 1.96, the identified trends are significant at the 95% confidence level. Positive values represent increasing trends and vice versa. The

MMK statistics of monthly standardized Surface Humid Index series in each month in the WRB are exhibited in Figure 2. The meteorological stations in Figure 2 are ranked based on the magnitude of their longitude, from west to east. Hence, the MMK statistics of standardized Surface Humid Index series in each month at 21 meteorological stations can reflect the spatiotemporal changes in monthly standardized Surface Humid Index series in the WRB. It can be clearly observed from Figure 2 that the trends of monthly standardized Surface Humid Index series show marked spatiotemporal characteristics. Specifically, in time dimension, the standardized Surface Humid Index in the WRB roughly exhibits statistically significant increasing trends in January, May, July, and December at the 95% confidence level, whilst that in February, April, and September shows statistically significant decreasing trends. In general, the standardized Surface Humid Index in the WRB has an obvious trend towards wetter condition in summer and winter, whereas that in spring and autumn has an obvious trend towards drier condition. In spatial dimension, the changes in monthly standardized Surface Humid Index series in the middle and eastern basin are more remarkable than those in the western basin.

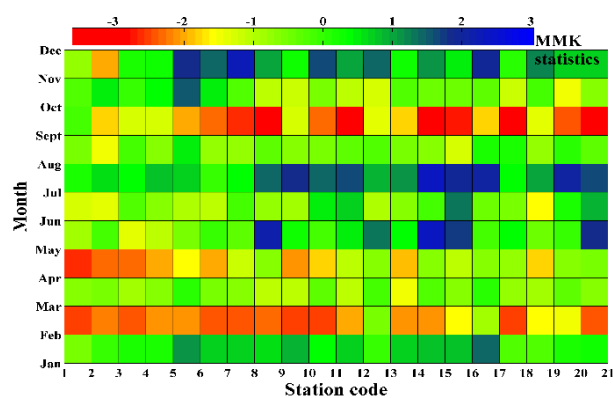


Figure 2. The MMK statistics of monthly standardized Surface Humid Index series in each month at 21 stations in the WRB.

Spatial Distribution Characteristics of the Extreme Dry and Wet Frequency in the WRB

Based on monthly standardized Surface Humid Index series at 21 meteorological stations in the WRB, the extreme dry and wet frequency in every year at these stations during 1960-2010 was calculated. Then, their mean extreme dry and wet frequencies are obtained. On the basis of the Inverse Distance Weighing (IDW) in the ArcGIS software, the spatial distribution of extreme dry and wet frequency in the WRB is plotted and shown in Figure 3. It can be obviously found from Figure 3A that the extreme wet frequency in the WRB exhibits a marked spatial discrepancy. Specifically, the northern basin has the highest extreme wet frequency, whilst the western basin has the lowest extreme wet frequency. Differently, the extreme dry frequency in the WRB shows a relatively small spatial discrepancy (Figure

3B). Generally, the extreme dry frequency in the western basin is smaller than that of other areas in the WRB.

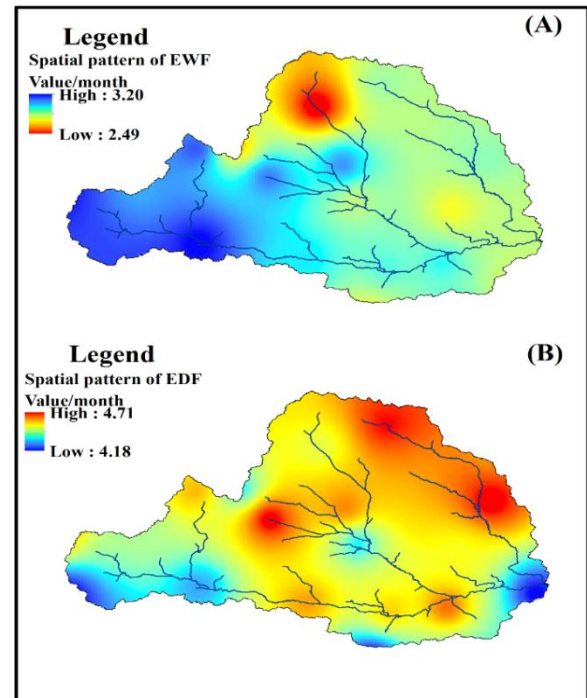


Figure 3. The spatial distribution of extreme wet (A) and dry (B) frequency in the WRB; EWF and EDF denote extreme wet frequency and extreme dry frequency, respectively.

Temporal Changes in the Extreme Dry and Wet Frequency in the WRB

The extreme dry and wet frequency in every year during 1960-2010 in the whole WRB was calculated, which is presented in Figure 4. It can be obviously seen from Figure 4 that the extreme dry frequency exhibits a slightly increasing trend, while the extreme wet frequency exhibits a slightly decreasing trend. Their corresponding MMK statistics are 0.77 and -1.13, respectively, indicating that both of them have no significant change at the 95% confidence level.

In addition, the MMK t was also used to compute the trends of the extreme dry and wet frequency in every year within 1960-2010 at the 21 meteorological station in the WRB. The spatial distribution of the MMK statistics of the extreme dry and wet frequency in the WRB is plotted and displayed in Figure 5. It can be seen from Figure 5A that the MMK statistics of the extreme wet frequency in the WRB have an obvious spatial difference. Specifically, the extreme wet frequency of the western basin and Huashan station located in the eastern basin exhibits a significant decreasing tendency at the 95% confidence level, whereas that in other areas in the WRB shows no significant trends. Generally, the decreasing extreme wet frequency of the western basin and Huashan station is

responsible for the slightly decreasing wet frequency in the whole basin outlined above. Compared with the extreme dry frequency, the MMK statistics of the extreme dry frequency in the WRB exhibit a relatively smaller spatial discrepancy (Figure 5B). The extreme dry frequency of some parts in the western basin and the Huashan station shows a significant increasing tendency at the 95% confidence level, whereas that in other areas in the WRB has no significant trends. In general, the increasing extreme dry frequency in these areas is responsible for the slightly increasing dry frequency in the whole basin outlined above.

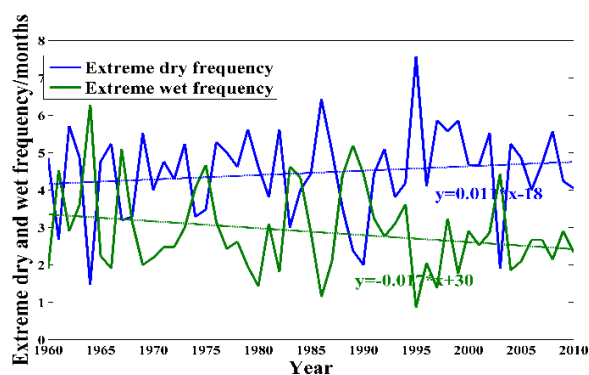


Figure 4. The extreme dry and wet frequency in every year during 1960-2010 in the whole WRB.

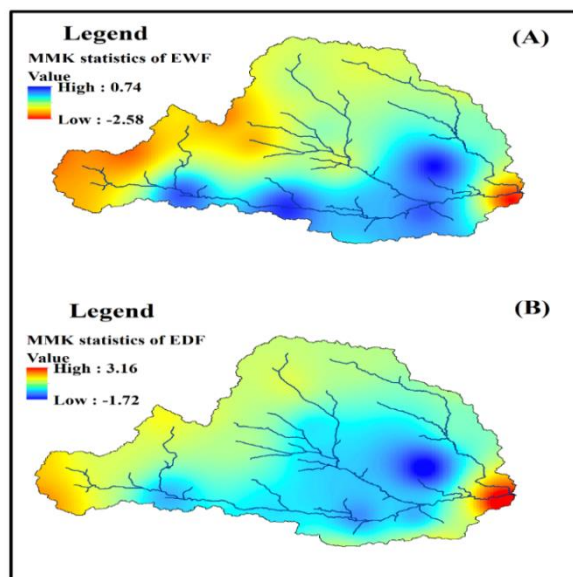


Figure 5. The spatial distribution of the MMK statistics of the extreme wet (A) and dry (B) frequency in the WRB; EWF and EDF denote extreme wet frequency and extreme dry frequency, respectively.

Identification of the Stationary of EDWE

Based on the heuristic segmentation method, possible change points in the extreme dry and wet frequency during 1960-2010 in the WRB were explored, thereby determining whether their stationarity is valid or not. The threshold P_0 was chosen as 0.95 and was selected as 25 in this present study (Pedro, Plamen and Lu \acute{s} , 2001). The detailed calculation steps can be referred to Huang *et al.* (2015a, 2016a). The results of change points in extreme dry and wet frequency series in the whole WRB are displayed in Figure 6. It can be clearly observed that no change point was identified due to the probability of their largest T is less than the threshold (P_0). Therefore, the stationarity of the extreme dry and wet frequency series is still valid.

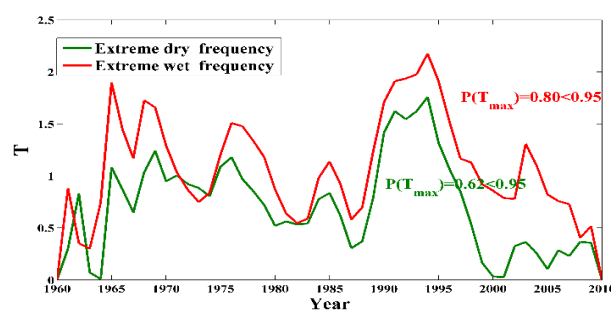


Figure 6. Identification of change points in extreme dry and wet frequency series in the whole WRB.

The Dry/Wet Conditions Period in the WRB

To analyze the dry/wet conditions period in the WRB, the wavelet analysis was adopted and the time-frequency distribution of the annual standardized Surface Humid Index in the whole WRB is exhibited in Figure 7. It can be clearly observed in Figure 7 that the dry/wet conditions in the WRB have a primary period of nearly 20 years and a secondary period of roughly 7 years, which is in line with the finding of Chen, Chang, and Huang (2014).

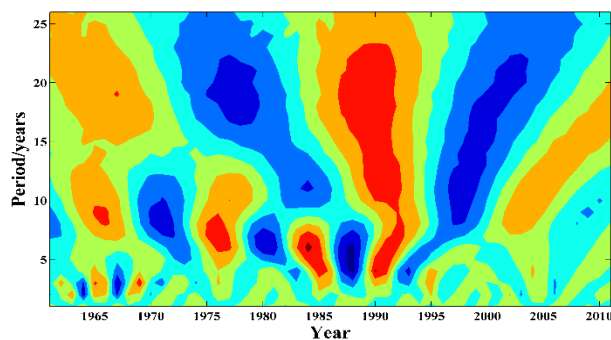


Figure 7. The time-frequency distribution of the annual standardized Surface Humid Index in the whole WRB.

DISCUSSION

Regional wet and dry events is considered to be related to the large-scale atmospheric circulation patterns, and attempts to explore the underlying physical mechanism may benefit the prediction of regional wet and dry events. Thus, the cross wavelet transform was applied to identifying correlations of H series with AMO, ENSO, PDO and NAO.

It can be found from Figure 8a that AMO exhibits a certain impact on annual standardized Surface Humid Index series in the WRB. Specifically, AMO shows significant negative linkages with annual standardized Surface Humid Index series with a signal of 2-4 year in 1960-1970. Additionally, it also exhibits significant positive linkages with annual standardized Surface Humid Index series with a signal of 8-9 year in 1985-1990. Generally, the cross wavelet phase angle has mean phase $130^{\circ} \pm 15^{\circ}$, meaning that H series has roughly 3 months lag compared with AMO in this period. Additionally, the wavelet coherence coefficients of H index and AMO were calculated, and the squared wavelet coherence of H series and AMO is presented in Figure 8b. It also shows the significant negative linkages between H series and AMO in 1960-1970 and significant positive linkages in 1980-1987.

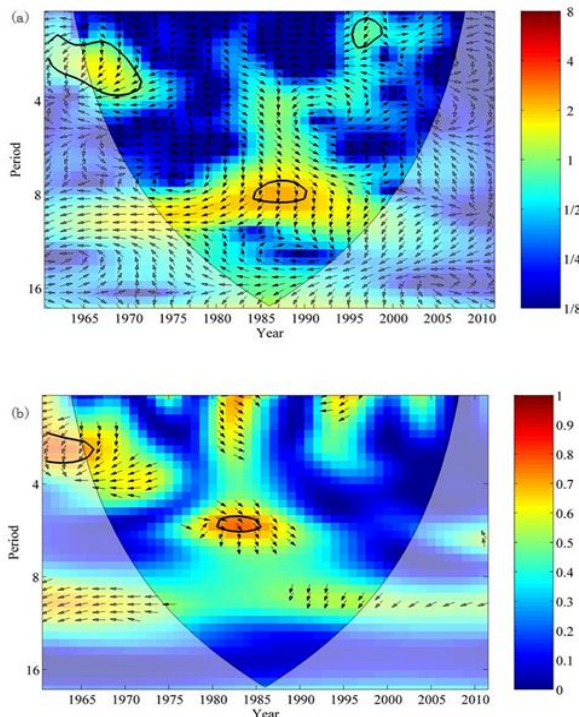


Figure 8. The cross wavelet transform (a) and wavelet coherence (b) maps of annual standardized Surface Humid Index series in the WRB and AMO in 1960-2010. The 5% confidence level against red noise is presented as a thick contour, and the relative phase linkage is represented as arrows, in which arrows pointing right stand for positive correlations, and arrows pointing left stand for negative correlations.

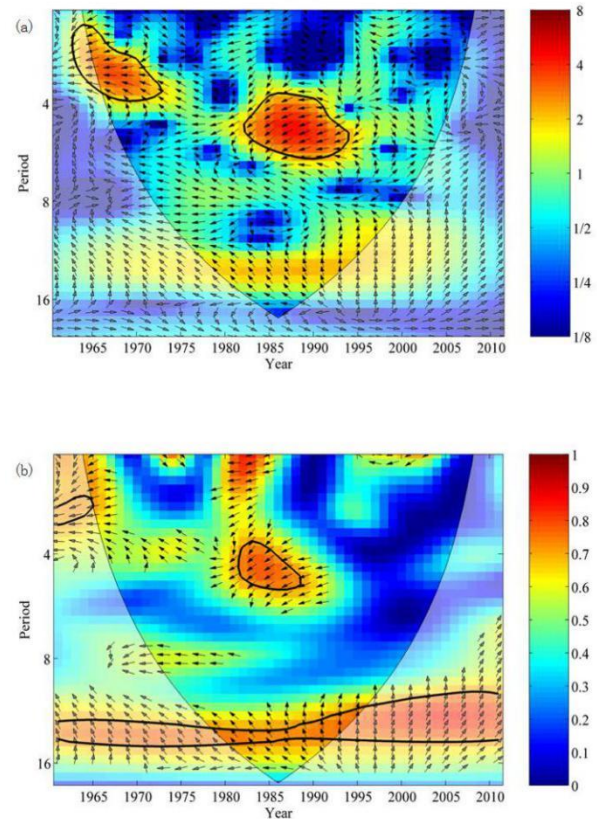


Figure 9. The cross wavelet transform (a) and wavelet coherence (b) maps of annual standardized Surface Humid Index series in the WRB and ENSO in 1960-2010.

It can be clearly observed from Figure 9a that ENSO exhibits strong impacts on annual standardized Surface Humid Index series in the WRB. Specifically, it shows statistically significant negative associations with annual standardized Surface Humid Index series with a signal of 2-4 year in 1960-1970 and a signal of 4-6 year in 1983-1994. The squared wavelet coherence of H series and ENSO shows more significant regions than cross wavelet transform, suggesting that ENSO exerts striking impacts on the changes in H series in the WRB (Figure 9b). PDO also shows strong impacts on annual standardized Surface Humid Index series in the WRB (Figure 10). Specifically, it shows statistically significant negative linkages with annual standardized Surface Humid Index series with a signal of 4-6 year in 1983-1994, which is a little similar with that of ENSO (Figure 10a). The squared wavelet coherence of H series and PDO also shows more significant regions than cross wavelet transform, suggesting that PDO exerts striking impacts on the changes in H series in the WRB (Figure 10b). Similarly, NAO also exhibits strong influences on annual standardized Surface Humid Index series in the WRB (Figure 11). Specifically, it has statistically significant positive relationships with annual

standardized Surface Humid Index series with a signal of 2-4 year in 1960-1970, which is contrary to that of AMO. Besides, it also shows significant positive linkages with annual standardized Surface Humid Index series with a signal of 4-5 year in 1991-1996 (Figure 11a). The squared wavelet coherence of H series and NAO also shows more significant regions than cross wavelet transform, suggesting that ENSO exerts obvious impacts on the changes in H series in the WRB (Figure 11b).

In general, among AMO, ENSO, PDO, and NAO, ENSO shows the strongest impacts on the EDWC in the WRB, followed by NAO and PDO, while AMO exhibits the weakest impacts on the EDWC in the WRB. Roughly, the large-scale atmospheric circulation patterns such as AMO, ENSO, PDO, and NAO strongly impact the changes in the EDWC in the WRB, which can effectively guide local hazards mitigation and water resources management.

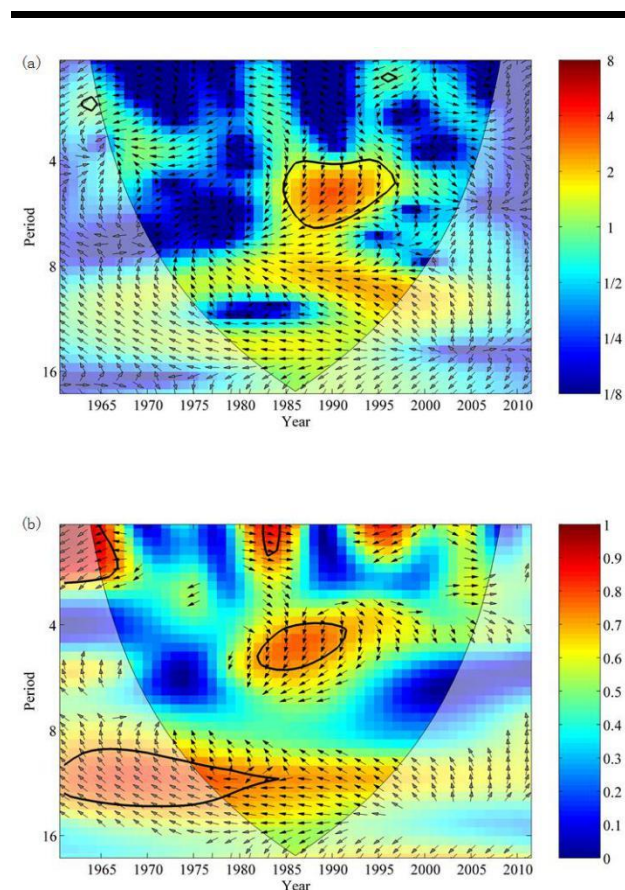


Figure 10. The cross wavelet transform (a) and wavelet coherence (b) maps map of annual standardized Surface Humid Index series in the WRB and PDO in 1960-2010.

Figure 3B shows that the calibration curve, plotting a graph of the electrode voltage versus the logarithmic ion concentration, was obtained in the experimental conditions described above. When the concentration increases, the electrode potential

becomes more negative since the phosphate microelectrode is sensing an anion. Three replicate measurements of each standard phosphate solution were made and the average values were used for calibration plots. It can be seen that no significant differences between plots were observed since the standard deviation values calculated were too small. The linear range was determined where the data points do not deviate from linearity by more than 10 mV. The potential response of the assembled phosphate ion-selective lab chip sensor showed a linear regression in the range of 1×10^{-5} to 1×10^{-3} M with a slope of 54 mV/decade. Thus, based on the calibration curve, the limit of the lower and upper detection was found to correspond to 1×10^{-6} M and 1×10^{-2} M at pH 6.0, respectively.

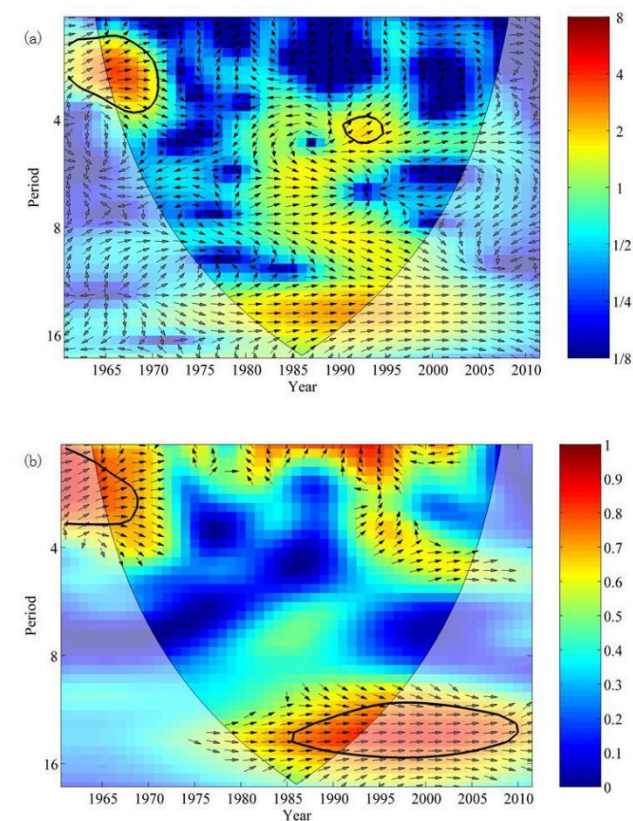


Figure 11. The cross wavelet transform (a) and wavelet coherence (b) maps of annual standardized Surface Humid Index series in the WRB and NAO in 1960-2010.

CONCLUSIONS

Investigation of the spatiotemporal changes in extreme wet and dry conditions and their correlations with planetary oscillations is very essential for regional hazards mitigation. In this study, a standardized Surface Humid Index was adopted to characterize EDWC. The MMK trend test approach and wavelet analysis was applied to calculate the trend and period of the EDWC in the WRB. The heuristic segmentation method was

adopted to explore the stationarity of extreme dry and wet frequency. Furthermore, the cross wavelet transform and coherence were used to examine the linkages between EDWC and four planetary oscillations. The main conclusions are presented below:

(1) The standardized Surface Humid Index in the WRB has a marked trend towards wetter condition in summer and winter, whereas that in spring and autumn has a striking trend towards drier condition. Generally, the changes in monthly standardized Surface Humid Index series in the middle and eastern basin are more remarkable than those in the western basin.

(2) The northern basin has the highest extreme wet frequency, whereas the western basin has the lowest extreme dry and wet frequency, and the spatial difference of the spatiotemporal changes in the extreme wet frequency is more obvious than that in the extreme dry frequency. Generally, the extreme dry frequency in the whole WRB shows a slightly increasing trend primarily owing to the significantly increasing extreme dry frequency of some parts in the western basin and the Huashan station, whilst the extreme wet frequency exhibits a slightly decreasing trend mainly due to the significantly decreasing extreme wet frequency of the western basin and Huashan station.

(3) The stationarity of the extreme dry and wet frequency series in the WRB is still valid. Its dry and wet conditions have a primary period of roughly 20 years and a secondary period of nearly 7 years.

(4) The large-scale atmospheric circulation patterns such as AMO, ENSO, PDO, and NAO strongly affect the EDWC in the WRB. ENSO shows the strongest impacts on the EDWC in the WRB, followed by NAO and PDO, while AMO exhibits the weakest impacts on its EDWC.

In conclusion, the findings in this study help to effectively guide local hazards mitigation.

ACKNOWLEDGMENTS

This research was supported by the National Natural Science Foundation of China (51709221), the Planning project of science and technology of water resources of Shaanxi (2017slkj-19), National Key R&D Program of China (2017YFC0405900), and Key laboratory research projects of education department of Shaanxi province (17JS104).

LITERATURE CITED

- Beniston, M. and Stephenson, D.B., 2004. Extreme climatic events and their evolution under changing climatic conditions. *Global and Planetary Change*, 44, 1-9.
- Cao, L.G.; Pan, S.M.; Wang, Q.; Wang, Y., and Xu, W., 2014. Changes in extreme wet events in Southwestern China in 1960-2011. *Quaternary International*, 321, 116-124.
- Chen, Y.T.; Chang, J.X., and Huang, S.Z., 2014. Variation characteristics of drought in Weihe River Basin based on Palmer drought severity index. *Journal of Natural Disasters*, 23(5), 29-37.
- Easterling, D.R.; Meehl, G.A.; Parmesan, C.; Changnon, S.A.; Karl, T.R., and Mearns, L.O., 2000. Climate extremes: Observations, modeling, and impacts. *Science*, 289(5487), 2068-2074.
- Fang, W.; Huang, Q.; Huang, S.Z.; Yang, J.; Meng, E.H., and Li, Y.Y., 2017. Optimal sizing of utility-scale photovoltaic power generation complementarily operating with hydropower: A case study of the world's largest hydro-photovoltaic plant. *Energy Conversion and Management*, 136, 161-172.
- Fang, W.; Huang, S.Z.; Huang, Q.; Huang, G.H.; Meng, E.H., and Luan, J.K., 2018. Reference evapotranspiration forecasting based on local meteorological and global climate information screened by partial mutual information. *Journal of Hydrology*, in press.
- Grinsted, A.; Moore, J.C., and Jevrejeva, S., 2004. Application of the cross wavelet transform and wavelet coherence to geophysical time series. *Nonlinear Processes in Geophysics*, 11, 561-566.
- Guo, J.L.; Guo, S.L.; Li, Y.; Chen, H., and Li, T.Y., 2013. Spatial and temporal variation of extreme precipitation indices in the Yangtze River Basin, China. *Stochastic Environmental Research and Risk Assessment*, 27, 459-475.
- Hamed, K.H. and Rao, A.R., 1998. A modified Mann-Kendall trend test for autocorrelated data. *Journal of Hydrology*, 204(1-4), 182-196.
- Huang, S.Z.; Chang, J.X.; Huang, Q., and Chen, Y.T., 2014a. Spatio-temporal changes and frequency analysis of drought in the Wei River Basin, China. *Water Resources Management*, 28(10), 3095-3110.
- Huang, S.Z.; Chang, J.X.; Huang, Q., and Chen, Y.T., 2015a. Identification of abrupt changes of the relationship between rainfall and runoff in the Wei River Basin, China. *Theoretical and Applied Climatology*, 120(1-2), 299-310.
- Huang, S.Z.; Chang, J.X.; Huang, Q.; Wang Y.M., and Chen, Y.T., 2014b. Spatio-temporal changes in potential evaporation based on entropy across the Wei River Basin. *Water Resources Management*, 28(13), 4599-4613.
- Huang, S.Z.; Hou, B.B.; Chang, J.X.; Huang, Q.; Chen Y.T., 2014c. Copulas-based probabilistic characterization of the combination of dry and wet conditions in the Guanzhong Plain, China. *Journal of Hydrology*, 519, 3204-3213.
- Huang, S.Z.; Huang, Q.; Chang, J.X.; Chen, Y.T.; Xing, L., and Xie, Y.Y., 2015b. Copulas-based drought evolution characteristics and risk evaluation in a typical arid and semi-arid region. *Water Resources Management*, 29, 1489-1503.
- Huang, S.Z.; Huang, Q.; Chang J.X., and Leng, G.Y., 2016a. Linkages between hydrological drought, climate indices and human activities: A case study in the Columbia River basin. *International Journal of Climatology*, 36(1), 280-290.
- Huang, S.Z.; Huang, Q.; Chen, Y.T.; Xing, L., and Leng, G.Y., 2015c. Spatial-temporal variation of precipitation concentration and structure in the Wei River Basin, China. *Theoretical and Applied Climatology*, 125(1), 67-77.
- Huang, S.Z.; Huang, Q.; Zhang, H.B.; Chen, Y.T., and Leng, G.Y., 2016b. Spatio-temporal changes in precipitation, temperature and their possibly changing relationship: a case

- study in the Wei River Basin, China. *International Journal of Climatology*, 36, 1160-1169.
- Hudgins, L.; Friehe, C.A., and Mayer, M.E., 1993. Wavelet transforms and atmospheric turbulence. *Physical Review Letters*, 71, 3279-3282.
- Jiang, C.; Xiong, L.; Xu, C.Y., and Guo, S.L., 2014. Bivariate frequency analysis of nonstationary low-flow series based on the time-varying copula. *Hydrological Processes*, 29(6), 1521-1534.
- Jones, P.D. and Moberg, A., 2003. Hemispheric and large-scale surface air temperature variations: An extensive revision and an update to 2001. *Journal of Climate*, 16(2), 206-223.
- Liu, S.Y.; Huang, S.Z.; Huang, Q.; Xie, Y.Y.; Leng, G.Y.; Luan, J.K.; Song, X.Y.; Wei, X., and Li, X.Y., 2017. Identification of the non-stationarity of extreme precipitation events and correlations with large-scale ocean-atmospheric circulation patterns: A case study in the Wei River Basin, China. *Journal of Hydrology*, 548, 184-195.
- Liu, S.Y.; Huang, S.Z.; Xie, Y.Y.; Leng, G.Y.; Huang, Q.; Wang, L., and Xue, Q., 2018. Spatial-temporal changes of rainfall erosivity in the loess plateau, China: Changing patterns, causes and implications. *Catena*, 166, 279-289.
- Ma, M.; Ren, L.; Singh, V.P.; Tu, X.; Jiang, S., and Liu, Y., 2015. Evaluation and application of the SPDI-JDI for droughts in Texas, USA. *Journal of Hydrology*, 521, 34-45.
- Ma, Z.G. and Fu, C.B., 2001. Trend of surface humid index in the arid area of northern China. *Acta Meteorologica Sinica*, 59(6), 737-746. (In Chinese)
- Ma, Z.G.; Hua, L.J., and Ren, X.B., 2003. The extreme dry/wet events in northern China during recent 100 years. *Acta Geographica Sinica*, 58, 69-74. (In Chinese)
- McKee, T.B.; Doesken, N.J., and Kliest, J., 1993. The relationship of drought frequency and duration to time scales. *Proceedings of the 8th Conference of Applied Climatology* (Anaheim, California), pp. 179-184.
- Meyer, S.J.; Hubbard, K.G., and Wilhite, D.A., 1993. A crop-specific drought index for corn: I. Model development and validation. *Agronomy Journal*, 85(2), 388-395.
- Monteith, J.L., 1965. Evaporation and environment. *Symposia of the Society for Experimental Biology*, 19, 205-234.
- Narasimhan, B. and Srinivasan, R., 2005. Development and evaluation of Soil Moisture Deficit Index (SMDI) and Evapotranspiration Deficit Index (ETDI) for agricultural drought monitoring. *Agricultural and Forest Meteorology*, 133, 69-88.
- Kam, J.; Sheffield, J., and Wood, E.F., 2014. Changes in drought risk over the contiguous United States (1901–2012): The influence of the Pacific and Atlantic Oceans. *Geophysical Research Letters*, 41, 5897-5903.
- Katz, R.W. and Brown, B.G., 1992. Extreme events in a changing climate: Variability is more important than averages. *Climatic Change*, 21(3), 289-302.
- Kiem, A.S. and Verdon-Kidd, D.C., 2009. Climatic drivers of Victorian streamflow: Is ENSO the dominant influence? *Australian Journal of Water Resources*, 13(1), 17-30.
- Palmer, W.C., 1965. *Meteorological Droughts*, U.S. Department of Commerce, Weather Bureau Research Paper 45, 58p.
- Pedro, B.G.; Plamen, C.I., and Lu ́, A.N.A., 2001. Scale invariance in the nonstationarity of human heart rate. *Physical Review Letters*, 87(16), 160815.
- Plummer, N.; Salinger, M.J.; Nicholls, N.; Suppiah, R.; Hennessy, K.J.; Leighton, R.M.; Trewin, B.; Page, C.M., and Lough, J.M., 1999. Changes in climate extremes over the Australian region and New Zealand during the twentieth century. *Climatic Change*, 42(1), 183-202.
- Reza, M.; Ali, S., and Donald, H.B., 2016. Changes of extreme drought and flood events in Iran. *Global and Planetary Change*, 144, 67-81.
- Sabziparvar, A.A.; Mirmasoudi, S.H.; Tabari, H.; Nazemosadat, M.J., and Maryanaji, Z., 2011. ENSO teleconnection impacts on reference evapotranspiration variability in some warm climates of Iran. *International Journal of Climatology*, 31(11), 1710-1723.
- Su, B.; Gemmer, M., and Jiang, T., 2008. Spatial and temporal variation of extreme precipitation over the Yangtze River Basin. *Quaternary International*, 186, 22-31.
- Talaei, P.H.; Tabari, H., and Ardakani, S.S., 2014. Hydrological drought in the west of Iran and possible association with large-scale atmospheric circulation patterns. *Hydrological Processes*, 28, 764-773.
- Tao, H.; Borth, H.; Fraedrich, K.; Su, B., and Zhu, X., 2014. Drought and wetness variability in the Tarim River Basin and connection to large-scale atmospheric circulation. *International Journal of Climatology*, 34, 2678-2684.
- Torrence, C. and Compo, G.P., 1998. A practical guide to wavelet analysis. *Bulletin of the American Meteorological Society*, 79(1), 61-78.
- Trenberth, K.E.; Dai, A.; van der Schrier, G.; Jones, P.D.; Barichivich, J.; Briffa, K.R., and Sheffield, J., 2014. Global warming and changes in drought. *Nature Climate Change*, 4(1), 17-22.
- Verdon-Kidd, D.C. and Kiem, A.S., 2015. Regime shifts in annual maximum rainfall across Australia - Implications for intensity-frequency-duration (IFD) relationships. *Hydrology and Earth System Sciences*, 19, 4735-4746.
- Vicente-Serrano, S.M.; Beguer ́, S., and L ́pez-Moreno, J.L., 2010a. A multiscale drought index sensitive to global warming: The standardized precipitation evapotranspiration index. *Journal of Climate*, 23(7), 1696-1718.
- Wang, B.; Zhang, M.; Wei, J.; Wang, S.; Li, S.; Ma, Q.; Li, X., and Pan, S., 2013. Changes in extreme events of temperature and precipitation over Xinjiang, northwest China, during 1960-2009. *Quaternary International*, 298, 141-151.
- Wang, S.; Jiao, S., and Xin, H., 2013. Spatio-temporal characteristics of temperature and precipitation in Sichuan Province, Southwestern China, 1960-2009. *Quaternary International*, 286, 103-115.
- Zhang, H.; Chen, Y.; Ren G., and Yang G., 2008. The characteristics of precipitation variation of Weihe River Basin in Shaanxi Province during recent 50 years. *Agricultural Research in the Arid Areas*, 26(4), 236-242. (In Chinese)
- Zhang, M.J.; He, J.Y.; Wang, B.L.; Wang, S.J.; Li, S.S.; Liu, W.L., and Ma, X.N., 2013. Extreme drought changes in

- Southwest China from 1960 to 2009. *Journal of Geographical Science*, 23(1), 3-16.
- Zhang, W.; Pan, S.M.; Cao, L.G.; Cai, X.; Zhang, K.X.; Xi, Y.H., and Xu, W., 2015a. Changes in extreme climate events in eastern China during 1960-2013: A case study of the Huaihe River Basin. *Quaternary International*, 380-381, 22-34.
- Zhang, Y.Q.; You, Q.L.; Lin, H.B., and Chen, C.C., 2015b. Analysis of dry/wet conditions in the Gan River Basin, China, and their association with large-scale atmospheric circulation. *Global and Planetary Change*, 133, 309-317.
- Zhao, J.; Huang, Q.; Chang, J.X.; Liu, D.F.; Huang, S.Z., and Shi, X.Y., 2015. Analysis of temporal and spatial trends of hydro-climatic variables in the Wei River Basin. *Environmental Research*, 139, 55-64.
- Zheng, J.; Wang, W.; Ge, Q.; Man, Z., and Zhang, P., 2006. Precipitation variability and extreme events in eastern China during the past 1500 years. *Terrestrial Atmospheric and Oceanic Sciences*, 17(3), 579.